

# Simulation Model for Solar Water Heating for Food Processing

**Dorota Wójcicka-Migasiuk**

Inst. of Fundamental Electrical Eng. and  
Electrotechnologies, Lublin Technical Univ.  
ul. Nadbystrzycka 38a, 20-618 Lublin, Poland tel:  
+4881 5381 292, fax: +4881 5381 289  
[dorotawm@eltecopol.lublin.pl](mailto:dorotawm@eltecopol.lublin.pl)

**Andrzej Chochoowski**

Electrical Energy Division,  
Warsaw Agricultural Academy,  
ul. Nowoursynowska 166, 02-787 Warsaw, Poland  
tel/fax: 4822 8439181  
[chochoowski@alpha.sggw.waw.pl](mailto:chochoowski@alpha.sggw.waw.pl)

## ABSTRACT

The paper presents uses of the Equivalent Thermal Network Method to formulate a mathematical model suitable for solar domestic hot water (SDHW) system analysis. Computer simulations using this model based on either weather conditions or varying system parameters can be done to show their influence on the system thermal performance. This approach should be useful to solar system designers. Transient analysis adds new aspects to the thermal performance of such systems not previously available. Comparisons with measurements taken on a real object prove the validity of the method for local conditions.

**Key words:** *solar heating, clean energy, SDHW system for food production processes, equivalent thermal network*

## INTRODUCTION

The effective use of solar energy presents opportunities for use of an alternative energy source which may in some cases have both an economic saving aspects and environment protection aspect. This is especially in environmentally sensitive areas. Healthy food production in rural areas is in the focus of interest of research carried out at many centers. This paper contributes to the application of solar energy in thermal applications.

It is comparatively easy to predict the hot water demand for a medium size food production plant (Recknagel-Sprenger, 1994; Mańkowski S., 1981; Carpenter JL., Vallis EA., Vranich AT., 1986.). To be considered for use a solar domestic hot water (SDHW) system

model, it must also predict the energy gain of the system (Duffie J.A., Beckman J.A., 1991). This paper presents the results of a very useful method for evaluation of the whole SDHW system combining solar collectors, pipelines, heat exchangers and accumulation, up to the water outlet points yielding 10% accuracy of temperature prediction for Central-East European climatic conditions.

The schematic layout of the SDHW system developed for this application is presented in figure 1 and the steady state model representation is given in figure 2. The most interesting point from the food production plant point of view is Node 6 the plant tap water intake. This is especially vital for the construction of a food production process procedure to take the advantage of this clean technology. It is important to decide when the hot water produced by the system can be used most effectively either to wash such products as fruits and vegetables or glass packaging. The model enables simulation along the whole flow path of both fluids.

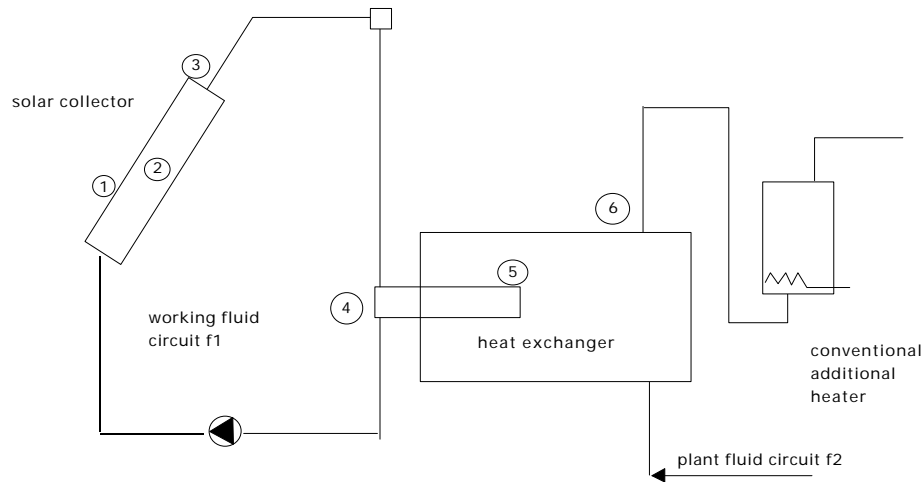


Fig. 1. SDHW system layout

## EQUIVALENT THERMAL NETWORK

The method, on which the simulation algorithms are based, is called the Equivalent Thermal Network - ETN (Chochowski A., 1991) and takes the advantage of the theory of analogy between the current flow in electric RC circuits and the heat transfer. The mathematical model is based on a numerical method called the Elementary Balance Method in which every element is represented by a node and relevant balance equations are formulated for them. The total thermal resistance of the whole node is expressed in units of °K/W. The method of describing the system shown in figure 1, in terms of thermal resistances for this study is shown in figure 2. This is the system of nodes and branches. There follows the list of what each node represents.

Node 1 –the collector glass cover of the mean temperature  $T_1$

Node 2 – the absorber of the mean temperature  $T_2$ ; the energy  $P_2$  is generated on its surface as the result of the irradiance passed through the cover

Node 3 –the working fluid in the collector of the mean temperature  $T_{f1}$

Node 4 –the working fluid in pipelines and in the heat exchanger

Node 5 – the heat exchange at the mean temperature  $T_5$  of the coil pipe

Node 6 –the plant fluid of the mean temperature  $T_{f2}$ , in which the heat power  $P_6$  (W) that can come from a conventional electric heater, can be focused

Branches express the heat transfer between two adjacent nodes. Thermal resistance symbols are the following:

$R_{1a}$  –collector glass cover to the ambience of the air temperature  $T_a$ ,

$R_{12}$  - collector glass cover to the absorber,

$R_{2a}$  - the absorber to the ambience through the collector housing,

$R_{23}$  - the absorber to the working fluid,

$R_{f1}$  – thermal resistance of the fluid (not indicated in the figure but, of course, included in the

system of equations describing the model),

$R_{40}$  - the piping system towards its ambience, which in this case, is the interior of a building/boiler room of temperature  $T_o$ ,

$R_{45}$  - the working fluid to the heat exchanger coil pipe of the mean temperature  $T_5$ ,

$R_{50}$  - the ambience inside the building to the heat exchanger coil pipe through the heat exchanger shell,

$R_{56}$  - the heat exchanger coil pipe to the plant fluid

$R_{12}$  - thermal resistance of the plant fluid

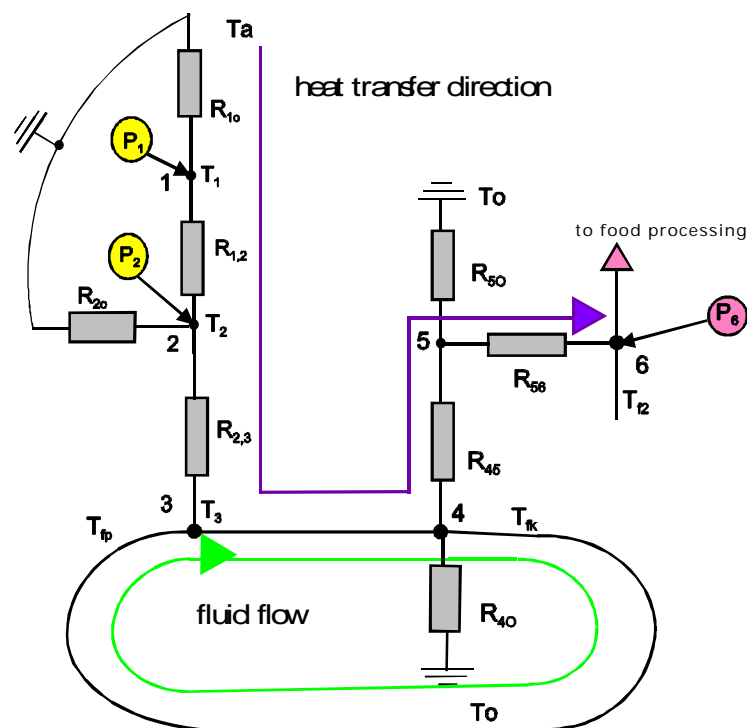


Fig. 2. Steady state model for the system shown in Fig.1

## STEADY STATE ANALYSIS

Figure 2 presents the model for the steady state analysis that is based on the system of heat balance equations in all nodes:

$$\begin{aligned}
 \text{Node 1: } & T_1 \left( \frac{1}{R_{1a}} + \frac{1}{R_{12}} \right) - \frac{T_2}{R_{1a}} = P_1 + \frac{T_a}{R_{12}} \\
 \text{Node 2: } & -\frac{T_1}{R_{12}} + T_2 \left( \frac{1}{R_{12}} + \frac{1}{R_{21a}} + \frac{1}{R_{23}} \right) - \frac{T_3}{R_{23}} = P_2 + \frac{T_a}{R_{2a}} \\
 \text{Node 3: } & -\frac{T_2}{R_{1a}} + T_3 \left( \frac{1}{R_{23}} + \frac{1}{R_{f1}} \right) + T_4 \left( \frac{1}{R_{45}} - \frac{1}{R_{f1}} + \frac{1}{R_{4o}} \right) - \frac{T_5}{R_{45}} = \frac{T_o}{R_{4o}} \\
 \text{Node 4: } & -\frac{T_2}{R_{23}} - T_3 \left( \frac{1}{R_{f1}} - \frac{1}{R_{23}} \right) + T_4 \left( \frac{1}{R_{45}} + \frac{1}{R_{f1}} + \frac{1}{R_{4o}} \right) - \frac{T_5}{R_{45}} = \frac{T_o}{R_{4o}} \\
 \text{Node 5: } & -\frac{T_4}{R_{45}} + T_5 \left( \frac{1}{R_{45}} + \frac{1}{R_{5o}} + \frac{1}{R_{56}} \right) - \frac{T_6}{R_{56}} = \frac{T_o}{R_{5o}} \\
 \text{Node 6: } & -\frac{T_5}{R_{56}} + T_6 \left( \frac{1}{R_{56}} + \frac{1}{R_{f2}} \right) = P_6 + \frac{T_{f2p}}{R_{f2}}
 \end{aligned}$$

This leads to a state matrix equation

$$\bar{T} = \Lambda^{-1} \bar{P} \quad (1)$$

where particular single column matrices are:

$$\text{temperature matrix : } \bar{T} = \begin{bmatrix} T_1 \\ T_2 \\ T_3 \\ T_4 \\ T_5 \\ T_6 \end{bmatrix}, \text{ input matrix: } \bar{P} = \begin{bmatrix} P_1 + \frac{T_a}{R_{1a}} \\ P_2 + \frac{T_a}{R_{2a}} \\ \frac{T_o}{R_{4o}} \\ \frac{T_o}{R_{4o}} \\ \frac{T_o}{R_{5o}} \\ P_6 + \frac{T_{f2p}}{R_{f2}} \end{bmatrix} \text{ and the state matrix } \Lambda \text{ is:}$$

$$\Lambda := \begin{bmatrix} \frac{1}{R_{1a}} + \frac{1}{R_{12}} & -\frac{1}{R_{12}} & 0 & 0 & 0 & 0 \\ -\frac{1}{R_{12}} & \frac{1}{R_{12}} + \frac{1}{R_{2a}} + \frac{1}{R_{23}} & -\frac{1}{R_{23}} & 0 & 0 & 0 \\ 0 & -\frac{1}{R_{23}} & \frac{1}{R_{23}} + \frac{1}{R_{f1}} & \frac{1}{R_{45}} - \frac{1}{R_{f1}} + \frac{1}{R_{40}} & -\frac{1}{R_{45}} & 0 \\ 0 & -\frac{1}{R_{23}} & \frac{1}{R_{23}} - \frac{1}{R_{f1}} & \frac{1}{R_{45}} + \frac{1}{R_{f1}} + \frac{1}{R_{40}} & -\frac{1}{R_{45}} & 0 \\ 0 & 0 & 0 & -\frac{1}{R_{45}} & \frac{1}{R_{50}} + \frac{1}{R_{56}} + \frac{1}{R_{45}} & -\frac{1}{R_{56}} \\ 0 & 0 & 0 & 0 & -\frac{1}{R_{56}} & \frac{1}{R_{56}} + \frac{1}{R_{12}} \end{bmatrix}$$

Particular rows in  $\bar{P}$  and  $\Lambda$  follow from thermal balance equations formulated for each node of ETN. The form of  $\Lambda$  gives an image of how the system of equations can be extended if additional nodes are incorporated into the system. Particular thermal resistances are computed in strict accordance to heat transfer through radiation, convection and conductance. Inputs P represent the supply of energy that comes from solar radiation understood as the product of irradiance i.e.: the energy gain from collectors in  $W/m^2$  and collector surface ( $m^2$ ). The example of steady state simulation results in all nodes (figure 3) shows the dependence on irradiance and gives the image of how temperatures in nodes change at different solar energy levels. The graph is plotted in relative values, i.e. relative to the values reached at the irradiance of  $650 W/m^2$ . Real values used to plot the graph are presented in Annex.

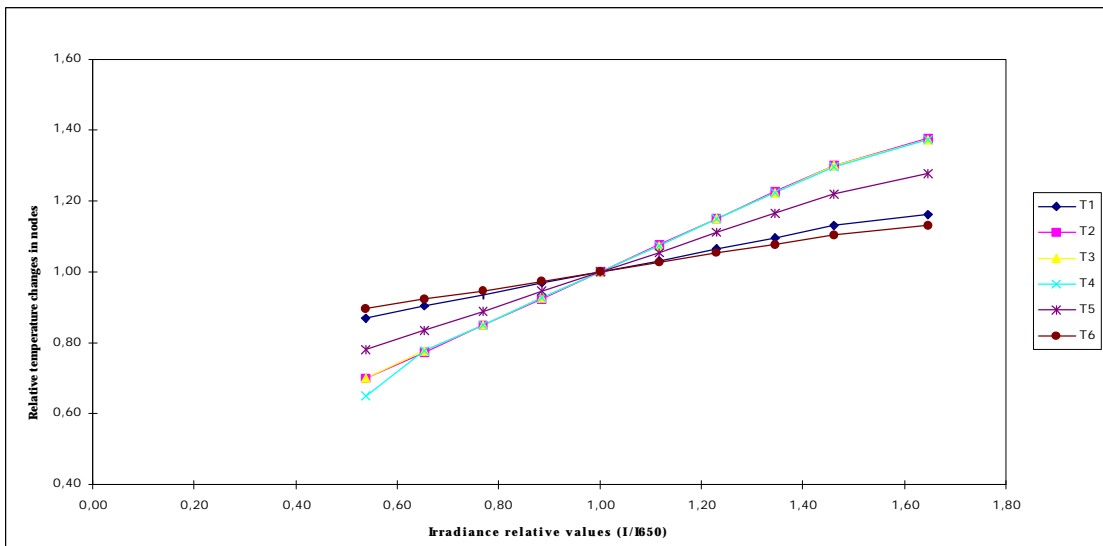


Fig. 3. The dependence of temperatures in Nodes 1 – 6 on irradiance at established ambient temperature 283 °K

### TRANSIENT ANALYSIS

The real dynamic nature of the system can not be presented through the steady state analysis. The inputs are always transient and because of thermal capacity is assigned to all nodes, the operation of the whole SDHW system is always transient. The basic equation describing the transient state is

$$\frac{d\bar{T}(t)}{dt} = -(\mathbf{c}^{-1}\mathbf{\Lambda}) \bar{T}(t) + \mathbf{c}^{-1} \bar{P}(t) \quad (2)$$

where  $\mathbf{c}$  is the thermal capacity matrix of all nodes.

The algorithms and the solution to this differential equation have been reached by standard MathCad 7.0 software. This solution is an exponential function of temperatures in all nodes:

$$T_i(t) = T_{pi}(0) + \sum_{i=1}^6 \Theta_{j,i} (1 - e^{-\frac{t}{t_i}}) \quad (3)$$

where:

$\Theta$  - temperature increase

$\tau$  - time constant.

Time constants are the point of interest in this paper. They control when after sunrise the process of real heating begins and when the heat accumulated in the volume of the heat exchanger can be effectively used.

The collectors must work for some time without introducing the working fluid to the plant fluid circuit. A second delay may be needed to allow the temperature to rise to a acceptable level for the exchange process. In the climatic conditions of central east European countries these time factors may decide if the system can operate without conventional heating, which is preferred, or how much of the additional power must be added to the system and when. The table below presents example time constants, response time and steady temperatures for particular nodes at established ambient conditions: irradiance  $I = 600 \text{ W/m}^2$  and ambient temperature  $T_a = 283 \text{ }^\circ\text{K}$ .

Figures 4 and 5 present an example of dynamics of the system. Figure 4 presents temperature curves for all nodes over a time period relevant to the response time.

Figure 5 presents the dynamics of Node 5. Because of its location inside the building, this node can either be cooled or heated. Its temperature can sometimes be higher than the ambient, especially in the morning. Given this condition, the operator must wait the time indicated by the graph when the temperature increase becomes positive before collector water can be led to the heat exchanger. The advantage of MathCad is that the graph of two changing function variables on horizontal axes can be plotted together as a quasi-spatial graph, however, the programme itself gives no possibility to properly describe each axis in it.

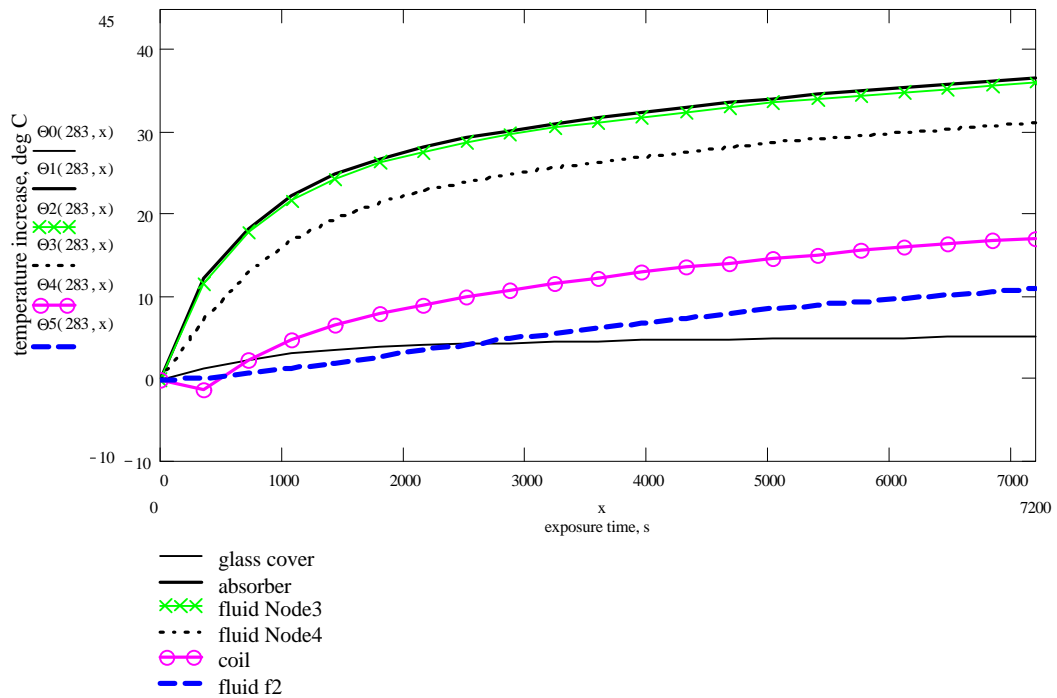
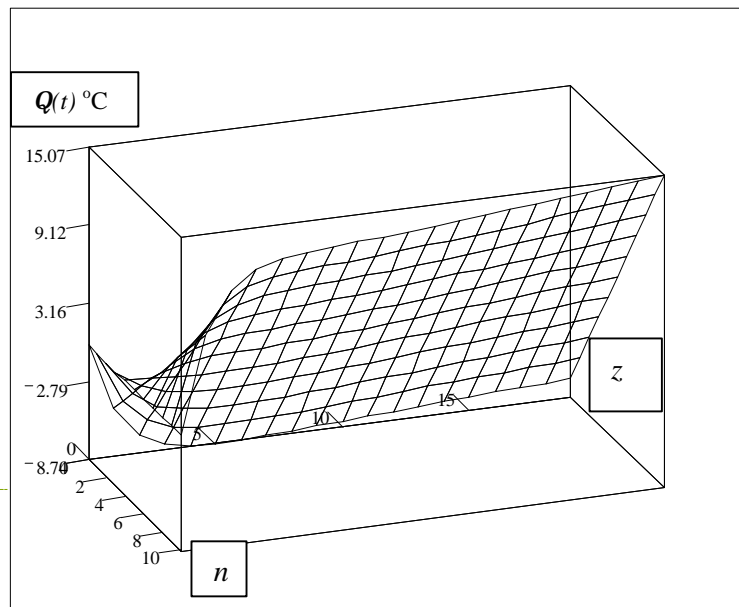


Fig. 4. Temperature increase curves for all nodes in first 7200 s from the starting point of simulation

$$z := 0..19 \quad t_z := z \cdot 5$$

$$M_{j,z} := K4(d43_j, t_z)$$



M

Fig. 5. Transient temperature increase  $\Theta(t)$  for the heat exchanger coil pipe, time period:0 to 190 s (in 20 substitutions every 10s) for 11 subsequent substitutions of ambient temperature of  $T_a: 273 + n \cdot 5 \text{ } ^\circ\text{K}$  ( $n = 0, 1 \dots 11$ ); the horizontal axis  $z$  is the time axis for  $z$  substitutions every 10 s

Table 1. Example time constants  $\tau$ , response time  $t_u$  ( $t_u \approx 3\tau$ ) and steady temperatures T for particular nodes

Node No	Node description	time constant $\tau$ (s)	steady temperatures T( °K)	response time $t_u$ (s)
<b>1</b>	collector cover	351	288.9	1053 (17.5 min)
<b>2</b>	absorber	5	325.6	15
<b>3</b>	working fluid Node 3	674	325.1	2022 (33.7 min)
<b>4</b>	working fluid Node 4	152	320.3	456 (7.6 min)
<b>5</b>	heat exchanger coil pipe	29	311.3	87
<b>6</b>	accumulated plant fluid	6200 (1.7 h)	300.2	18600 (5.2 h)

### MEASURING SYSTEM

The system combines two collector of total surface 3 m<sup>2</sup> and a heat exchanger of 150 dm<sup>3</sup>.

The measurements in a tested plant combining all elements indicated in figure 1 were taken automatically. Measurement and Data Acquisition System comprised:

- Kipp & Zonnen paranometer CM3 to measure total solar radiation intensity on the collector surface;
- Semiconductor temperature sensors - ambient temperature, ambient temperature in the heat exchanger room, fluid temperature in the outflow from collectors (Node 3), fluid temperature flowing into the heat exchanger coil, outflow from the heat exchanger (Node 6);
- Pulse flowmeter measured flow capacity;
- Measuring card Advanteh 818,

- Computer PC with software Genie.

Measurements were taken between April 1995 and October 1998. Figure 6 shows temperature and irradiance measurements taken on 95.09.09 in the ambience and in the outflow from collectors and temperature simulation in Node 3. Figure 7 shows two graphs – Tcol/T3 that results directly from figure 6 and Tf2/T6 that was determined in the same way but for Node 6.

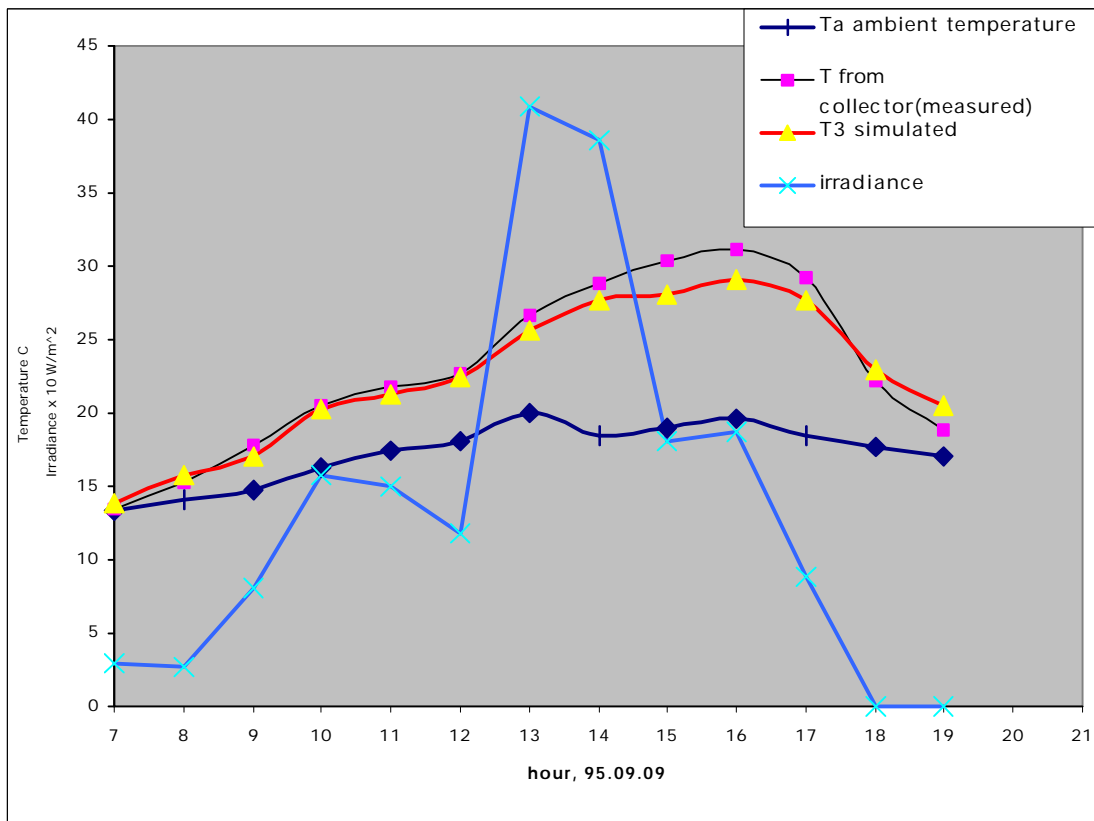


Fig. 6. Measurements taken in the ambience and in outlet from collectors and the simulation of Node 3

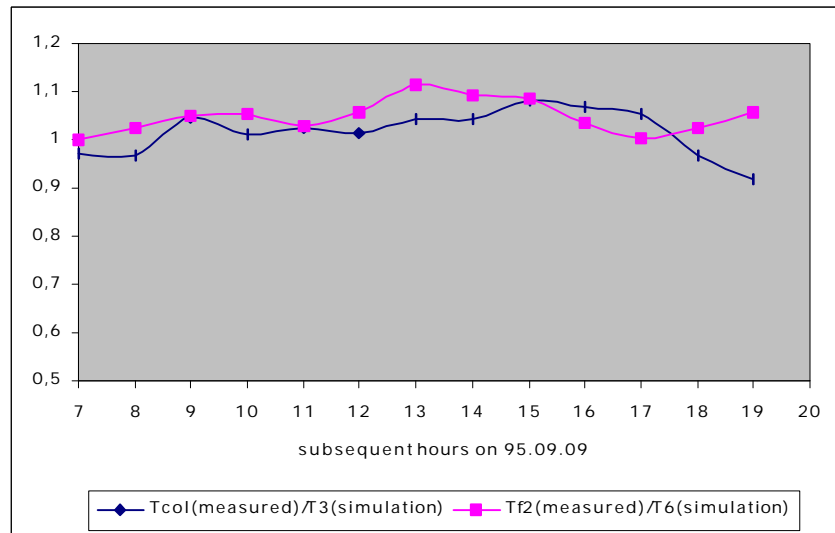


Fig.6. Comparison between measured and simulated values at Node 3 and Node 6

Another example graph can give reasons for good conclusions, i.e. the graph of coincidence between simulated values and measurements (fig. 7). This comparison proves that the simulation model is reliable and can be very useful to design SDHW systems and predict their short and long – term performance. The difference between measured and simulated values is maintained within 10%.

## CONCLUSIONS

The main conclusion is that the simulation model reflects real transient temperatures in nodes properly enough and thus can be useful for designers of such solar systems.

Simulations shown in figures 4 and 5 indicate on the dynamic of temperature in nodes which means that it must be considered when the operation of systems is planned.

These solar system are recommended for use in environmentally sensitive areas and because of their simplicity are specially recommended for developing rural regions.

## REFERENCES

- Duffie J.A., Beckman J.A., 1991. Solar Engineering of Thermal Processes. John Wiley and Sons, New York.
- Recknagel-Sprenger, 1994. Heating and Air - Conditioning. Guide. (in Polish) EWFE – Gdańsk.
- Mańkowski S., 1981. Hot water system (in Polish) Arkady W-wa.
- Carpenter J.L., Vallis E.A., Vranich A.T., 1986. Performance of a UK Dairy Solar Water Heater, Journal of Agricultural Engineering Resources vol. 35, ss. 131-139.
- Chochowski A., 1991. Thermal state analysis for flat plate solar collectors. SGGW W-wa (in Polish)
- Lagasse J., 1965. Electric Circuit Theory WNT W-wa (in Polish)
- Chochowski A., Wójcicka – Migasiuk D., 1998. Equivalent network method in steady state analysis of hot water plants incorporating solar collectors in dairies, - abstract- 3rd Int. Conference "Physics of Agro and Food Products", 24, Inst. Agrofizyki PAN, Lublin.

## APPENDIX

### Values used to plot the graph in figure 3:

Temp. °C: Increase reached at subsequent irradiance						Subsequent Irradiance
T1	T2	T3	T4	T5	T6	
12,4906	26,1839	25,8458	24,0000	19,5354	12,5112	350,00
12,9548	29,0111	28,5965	28,5965	20,9137	12,8742	425,00
13,4189	31,8382	31,3472	31,3472	22,2920	13,2371	500,00
13,8830	34,6654	34,0979	34,0979	23,6703	13,6001	575,00
14,3471	37,4925	36,8486	36,8486	25,0486	13,9631	650,00
14,8113	40,3197	39,5993	39,5993	26,4269	14,3261	725,00
15,2754	43,1468	42,3500	42,3500	27,8053	14,6891	800,00
15,7395	45,9740	45,1007	45,1007	29,1836	15,0521	875,00
16,2036	48,8011	47,8514	47,8000	30,5619	15,4151	950,00
16,6678	51,6283	50,6021	50,6021	31,9402	15,7780	1071,00
Relative temperature increase: reached temperature to the temperature increase reached at irradiance I = 650 W/m <sup>2</sup>						
0,54	0,8706	0,6984	0,7014	0,6513	0,7799	
0,65	0,9030	0,7738	0,7761	0,7761	0,8349	
0,77	0,9353	0,8492	0,8507	0,8507	0,8899	
0,88	0,9677	0,9246	0,9254	0,9254	0,9450	
1,00	1,0000	1,0000	1,0000	1,0000	1,0000	
1,12	1,0323	1,0754	1,0746	1,0746	1,0550	
1,23	1,0647	1,1508	1,1493	1,1493	1,1101	
1,35	1,0970	1,2262	1,2239	1,2239	1,1651	
1,46	1,1294	1,3016	1,2986	1,2972	1,2201	
1,65	1,1617	1,3770	1,3732	1,3732	1,2751	

## List of figure captions

- 1 Fig. 1. SDHW system layout
- 2 Fig. 2. Steady state model for the system shown in Fig.1
- 3 Fig. 3. The dependence of temperatures in Nodes 1 – 6 on irradiance at established ambient temperature 283 °K
- 4 Fig. 4. Temperature increase curves for all nodes in first 7200 s from the starting point of simulation
- 5 Fig. 5. Transient temperature increase  $\Delta T(t)$  for the heat exchanger coil pipe, time period: 0 to 190 s (in 20 substitutions every 10s) for 11 subsequent substitutions of ambient temperature of  $T_a: 273 + n \cdot 5 \text{ °K}$  ( $n = 0, 1 \dots 11$ ); the horizontal axis  $z$  is the time axis for  $z$  substitutions every 10 s
- 6 Fig.6. Measurements taken in the ambience and in outlet from collectors and the simulation of Node 3
- 7 Fig. 7. Comparison between measured and simulated values at Node 3 and Node 6